Description of Peripheral Collisions of Heavy Ions at Fermi Energies with Transport Approach

T.I. Mikhailova[1], B. Erdemchimeg[2,3], A.G. Artyukh[2], S.M. Lukyanov[2], Yu.M. Sereda[2,4], M. Di Toro[5], H.H. Wolter[6]

e-mail: tmikh@jinr.ru, [1]Laboratory of Information Technologies, JINR, Dubna

[2]Flerov Laboratory of Nuclear Reactions, JINR, Dubna

[3]Mongolian National University, NRC, P.O.B 46A/305, Ulaan Baatar, Mongolia

[4]Institute for Nuclear Research NAS, 252650, prospect Nauki 47, Kyiv-22, Ukraine

[5]Lab. Naz. del Sud, INFN, I-95123 Catania, Italy

[6]Faculty of Physics, University of Munich, 85748 Garching, Germany

Fragmentation reactions are of importance for the production of secondary unstable beams in heavy ion collisions. At Fermi energies the mechanism is between that of dissipative, deep-inelastic collisions and direct breakup processes characteristic of higher energies and the experimental data show features of both, e.g. in the asymmetric shape of the velocity spectra of the detected fragments. Different models are used to describe these type of reactions. These are emprirical fragmentstion models (EPAX [1], abrasion-ablation models [2], phase space parametrization models (HIPSE [3], and semi-classical transport models of the Boltzmann-Vlasov type [4]. In this contribution,we use this latter approach using the non-relativistic BNV code developed in Catania [5] and optimized in Dubna [6, 7]. This code has been used previously to interpret experimental data mesured in Dubna at the FLNR with the COMBAS forward spectrometer [8]. here BNV calculations for two reactions are presented ^{40}Ar on ^{8}Be (inverse kinematics) and ^{40}Ar on ^{181}Ta (direct kinematics) at $E/A = 57$ MeV, for which rather detailed data (including interpretations in the above models, except transport models) exist [9]. The dynamics of the two reactions are compared, together with the excitation energies of the projectile-like primary fragments. We analyze velocity and isotope distributions of projectile-like fragments in the reactions ^{40}Ar on ^{181}Ta at $E/A = 57$ MeV collisions. To compare with the experimental data we decompose the asymmetric experimental velocity distributions into two components [6]: a component centered at beam velocity (called direct or breakup, BU) and a dissipative or deep-inelastic component (DIC), that peaks at velocities below beam velocity. We find that in the semi-classical transport theory only the dissipative component is reproduced. The direct component has been interpreted in the Goldhaber model [10], and its width follows the general predictions of this model.

We first give a brief describtion of the transport appraoch used in this work. The Boltzmann-Nordheim-Vlasov (BNV) transport approach describes the time evolution of the one-body phase space distribution function $f(\mathbf{r}, \mathbf{p}, t)$ under the influence of a Vlasov mean field $U(f)$ and a Boltzmann two-body collision term I_{cls}, which includes the effect of Pauli blocking (Nordheim or Uehling-Uhlenbeck collision term)[4]

$$\frac{\partial f}{\partial t} + \frac{\vec{p}}{m}\nabla_{\vec{r}}f - \nabla_{\vec{r}}U\nabla_{\vec{p}}f = I_{cls}. \quad (1)$$

Here m is the nucleon mass. The potential $U(f)$ used in our calculations is the sum of a isoscalar mean field potential of the Skyrme type [5], a nuclear symmetry potential, and the Coulomb potential. The solution of the non-linear integro-differential eqs.(1) is achieved by simulations using the test-particle method [4]. In this method the distribution function $f(\vec{r}, \vec{p}, t)$ is represented as a sum of contributions of test particles, distributed over the volume of the system, having velocities in the local Fermi sphere:

$$f(\vec{r}, \vec{p}) \cong \frac{1}{NA}\sum_i g(\vec{r} - \vec{r}_i(t))\, \tilde{g}(\vec{p} - \vec{p}_i(t)) \quad . \quad (2)$$

The quantities $\vec{r}_i$, $\vec{p}_i$ are the positions and momenta of the test particles i, moving in time, and the functions g and $\tilde{g}$ describe the shape of a test particle distribution in coordinate and momentum space. N is the number of test particles per nucleon, which is of the order of 50 to 100. In our approach we use for the shape functions triangle distributions instead of more common gaussians to save the time in the calculations. Thus the distribution function for a nucleus of mass A is represented as a sum of NA test particles. Test particles also carry an index for isospin, such that protons and neutrons can be distinguished.

It can be shown [4] that between collisions the test particles propagate according to Hamilton equations of motion

$$\frac{\partial \vec{p}_i}{\partial t} = -\nabla_r U(\vec{r}_i, t) \quad ; \quad \frac{\partial \vec{r}_i}{\partial t} = \vec{p}_i/m \quad . \quad (3)$$
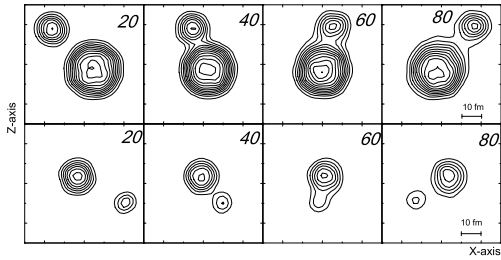
Figure 1: (left) Density distribution integrated over Y-axes for the collision of ^{40}Ar on ^{181}Ta at E/A = 57 MeV for different time steps. (right) Density distribution integrated over Y-axes for the collision of ^{40}Ar on ^{8}Be at E/A = 57 MeV for different time steps.

Figure 2: Excitation energy per nucleon for the reaction ^{40}Ar on ^{181}Ta at E/A = 57 MeV (solid curve), and ^{40}Ar on ^{8}Be (dashed curve) as a function of $b/(R_{tar} + R_{proj}$.

The collision term is treated in a stochastic way, choosing the collision probability according to the total cross section, and the collision angle according to the angular dependence. To start the solution of the set of eqs.(3) for colliding nuclei of the mass A_1, A_2, charge Z_1, Z_2, the initial coordinates r_i and the momenta p_i of all test-particles are found. Then the collision for kinetic energy $Ekin$ and impact parameter b is set up. The propagation of the test particles is a Cauchy problem solved numerically with the Euler-Richardson algorithm in which the momenta are shifted by a half-time step as compared to position evaluation. The positions of r_i and p_i are output with a time interval of 10 fm/c to be able to follow the dynamics of the collision.

From the test particle positions r_i and p_i the distribution function $f(r, p, t)$ is determined as in eqs.(2) and the expressions

$$n(r,t) = \int f(r,p,t)\, d\vec{p} \quad ; \quad \vec{u}(r,t) = \frac{1}{m} \int \vec{p} f(r,p,t)\, d\vec{p}$$
(4)

give the mean local number density $n(r,t)$ and collective velocity $\vec{u}(r,t)$ of the distribution. The time evolution of the test particles is continued until the freeze-out time. We define the freeze-out time as a minimal time when different fragments comprising the system are sufficiently isolated from each other so that nuclear forces between them are negligible. In these reactions this is about 100 fm/c for peripheral reactions, depending on the impact parameter of the reaction. At freeze-out the state of the system can be characterized as a collection of primary fragments with different A and Z, positions, momenta and intrinsic energy E_{in}. One has to employ a cluster recognition algorithm to identify the fragments. In this work we used a simple cut-off method in coordinate space, so that all test-particles inside a contour with this cut-off density form a fragment.
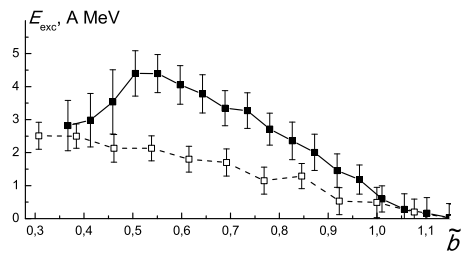
In fig.1 density distributions in the x-z plane (re-action plane) are shown for the reactions ^{40}Ar on ^{181}Ta at E/A = 57 MeV for impact parameter b= 10 fm and A^{40}Ar on ^{8}Be at the same energy at b=6 fm, respectively. The values of impact parameter b for two reactions are chosen so that the reduced impact parameter $\tilde{b} = b/(R_{tar} + R_{proj})$ is the same, where R_{tar} and R_{proj} are the radii of the target and projectile. One can see that in the case of the Ta target the nuclear interaction is stronger and the two nuclei form a connected system for the longer period of time. As a result the influence of the collision on the projectile-like fragment (nucleon loss and energy dissipation) is larger in the case of direct ($A_{tar} > A_{proj}$) in comparison with inverse kinematics ($A_{tar} < A_{proj}$).

Transport model calculations yield the values of the intrinsic energy of each fragment as $E_{in} = E_{mf} + E_{sym} + E_{coul}^{in} + E_{kin}^{fermi}$, where E_{mf} is the isoscalar mean field potential energy, E_{sym} the symmetry energy, E_{coul}^{in} the intrinsic coulomb energy, and E_{kin}^{fermi} the kinetic energy of the Fermi motion of the nucleons in the nucleus. The fragments produced in the transport calculation at the freeze-out configuration are still considerably excited. I.e, the intrinsic energy of the fragment is higher than the ground state energy E_{ground} for the an isotope with the same values of A and Z projected in time until $t = t_{freeze-out}$ without a collision. Then we calculate the excitation energy of the fragment $E_{exc} = (E_{in} - E_{ground})$.

The excitation energies per nucleon for the two reactions ^{40}Ar on ^{181}Ta and A^{40}Ar on ^{8}B at E/A = 57 MeV are shown in fig.2 as a function of the normalized impact parameter $b/(R_{tar} + R_{proj})$. As was mentioned in the discussion of fig. 1 the interaction between target and projectile is stronger the heavier is the target, which is seen to result in a higher

excitation energy. Also the range of impact parameters at which a binary reaction occurs is larger in the case of the heavy target, which will be seen to result in a larger range of produced isotopes.

The excited fragments at freeze-out will de-excite also by evaporating further particles before detection. This secondary evaporation has to be taken into account when comparing to experimental data. To investigate the effect of this secondary evaporation on the velocity spectra and isotope distributions we use the Statistical Multifragmentation Model (SMM) by Bondorf, Mishustin and Botvina[11]. Besides the mass and charge of the excited fragment, this model uses critically its excitation energy as specified above. We also show the dispersion of the excitation energy over many calculated events. The evaporation has considerable influence on the final isotope distributions and velocity spectra.

Results of the calculation are shown in fig. 3 for the reactions ^{40}Ar on ^{181}Ta at $E/A = 57$ MeV and ^{40}Ar on ^{8}Be at the same energy for mass distributions and in fig. 4 for velocity distributions. These are compared with the experimental data from ref.[9]. In the fig. 3 the isotope distributions of the projectile like fragments are shown. Our calculations overestimate the yields for the heavy fragments but give rather good predictions for lighter isotopes in case of Ta target. For light target Be the agreement is not so good. This maybe connect with the underestimation of dissipation in our calculations in the case of Be target.

In the fig.4 we show the calculated velocity distributions (solid curves) in comparison with experiment (dashed curves). Obviously the calculations are not able to reproduce the part of the spectra with velocities at or higher than the beam velocity. We conclude, as already found in previous studies [7] that the transport approach describes only the dissipative part of peripheral collision. We determine the dissipative part, by subtracting from the experimental spectra a (symmetric) Gaussian fitted to the high velocity part of the spectrum. We consider the residual, shown in fig 4 as a dotted curve with , as the dissipative component and compare it to the calculations The position of the calculated velocity spectra agrees fairly well with the position of the above determined dissipative experimental spectrum for the reaction ^{40}Ar on ^{181}Ta, but are shifted to the right for the light target. This again is a result of rather small value of excitation energy for the case of ^{40}Ar on ^{8}Be. We will study this question more thoroughly in our future work. We have studied a Fermi energy heavy ion collision using the BNV transport model approach ref.[12]. We have compared fragment isotope distributions and fragment velocity spectra to experimental data in the
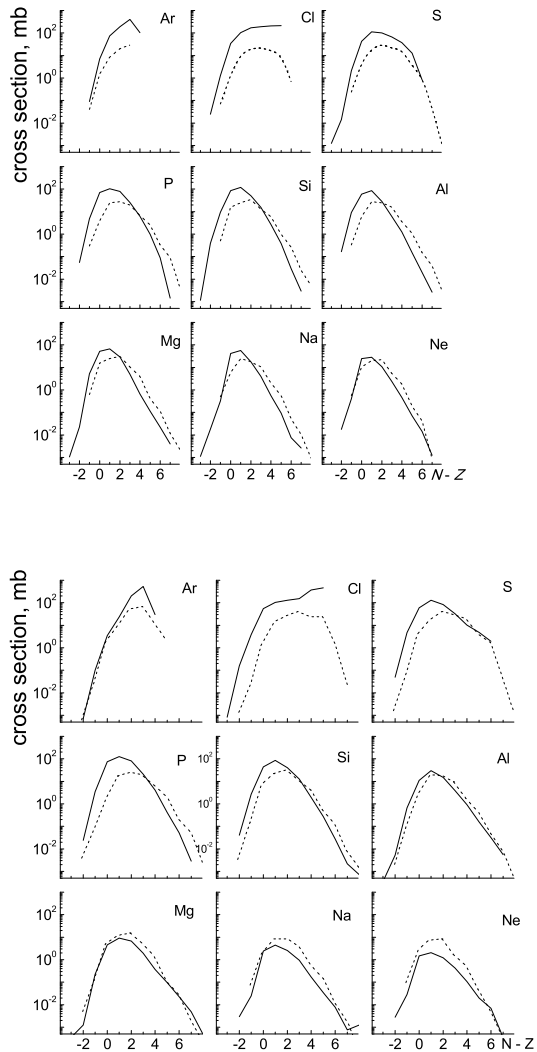

Figure 3: (left) Isotope mass distribution for some elements for the reaction ^{40}Ar on ^{181}Ta at $E/A = 57$ MeV, (right) and ^{40}Ar on ^{8}Be at the same energy. The signatures are: calculations - solid line, experiment [9]- dashed line

literature. In doing so we take into account the secondary de-excitation of the primary fragments in statistical model, calculating the excitation energy consistently with the transport model. These had previously been interpreted with different phenomenological models for fragmentation reactions. It is seen that the transport model, which has no empirical parameters adjusted to the fragmentation reaction, describes the data reasonably well. This is, however, only the case, if we consider the dissipative part of the reaction. The direct part, which is most likely due to multi-nucleon transfer direct reactions, and which is centered around the beam velocity, is

Figure 4: (left) Velocity distributions distribution for some elements for the reaction ^{40}Ar on ^{181}Ta at $E/A = 57$ MeV, (right) and ^{40}Ar on ^{8}Be at the same energy. The signatures are: calculations - solid line, experiment [9]- dashed line

not reproduced in a transport model, as expected. It is also seen, that the study of velocity distributions, which is usually not found in the literature, is critical in understanding the reaction mechanism to which it is much more sensitive. Further studies of the fragmentation processes are desirable, both in view of the physical understanding and in view of the practical importance in the production of radioactive beams. The results of a recent experiment of A^{40}Ar on ^{8}B at $E/A = 36$ MeV conducted at the FLNR in Dubna [13] are being processed and will be useful to answer these questions.

References

[1] K. Sümmerer, B. Blank, *Phys. Rev.* C 61, 034607 (2000).

[2] J.D. Bowman, W.J. Swiatecki, C.F. Tsang, *LBL Report* LBL-2908 (1973).

[3] D. Lacroix, A.V. Lauwe, D. Durand, *Phys. Rev.* C 69, 054604 (2004).

[4] G.F. Bertsch and S. Das Gupta, *Phys. Rep.*, **160** (1988) 189.

[5] V. Baran et al., *Phys. Rep.* **410** (2005) 335.

[6] T. Mikhailova et al., *Romanian Jour. Physics*, **52**, 857 (2007).

[7] T. I. Mikhailova, Bull. Russian Academy of Sciences. Physics, **75** (2011) 1511.

[8] A.G. Artukh et al., *Yad. Phys.* **65** (2002) 419.

[9] X. H.Zhang et al., Phys. Rev. C 85 (2012) 024621

[10] A.S. Goldhaber, *Phys. Lett.* **B53** (1974) 306.

[11] J.P. Bondorf et al., *Phys. Rep.* **257** (1995) 133.

[12] reports to the conferences MMPC13 and NUCLEUS-2013

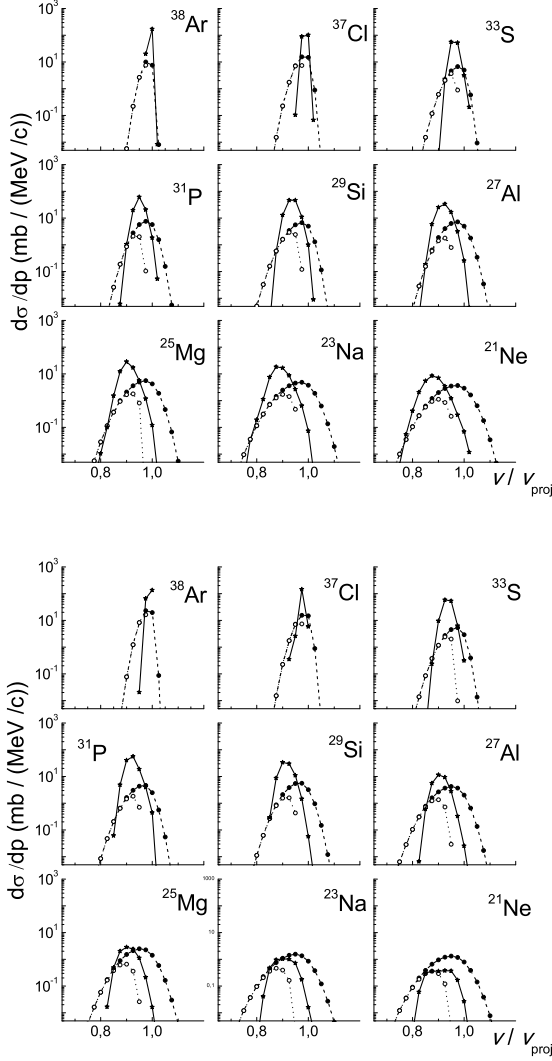[13] Yu. M. Sereda et al., Preprint JINR P7-2013-90, submitted to Phys. Atom. Nucl